Enhancing luminous flux and color rendering of laser-excited YAG:Ce^{3+} single crystal phosphor plate via surface roughening and low-temperature sintering a $CaAlSiN_3$:Eu^{2+} phosphor-in-borate glass

Wei Chen, Chen; Cao, Dunhua; Dong, Yongjun; Xiong, Jingkang; Trofimov, Yuri; Lishik, Sergey; Zhang, Guoqi; Fan, Jiajie

DOI
10.1016/j.jlumin.2022.119225

Publication date
2022

Document Version
Final published version

Published in
Journal of Luminescence

Journal of Luminescence 251 (2022) 119225

Contents lists available at ScienceDirect

Journal of Luminescence

journal homepage: www.elsevier.com/locate/jlumin

Full Length Article

Enhancing luminous flux and color rendering of laser-excited YAG:Ce^{3+} single crystal phosphor plate via surface roughening and low-temperature sintering a $CaAlSiN_3$:Eu^{2+} phosphor-in-borate glass

Wei Chen [a,c], Dunhua Cao [d], Yongjun Dong [d], Jingkang Xiong [c], Yuri Trofimov [e], Sergey Lishik [e], Guoqi Zhang [f], Jiajie Fan [a,b,c,f,g,*]

[a] Institute of Future Lighting, Academy for Engineering & Technology, Fudan University, Shanghai, 200433, China
[b] State Key Laboratory of Applied Optics,Changchun Institute of Optics, Fine Mechanics and Physics, Chinese Academy of Sciences, Changchun, 130033, China
[c] Changzhou Institute of Technology Research for Solid State Lighting, Changzhou, 213164, China
[d] Nanjing Crylink Photonics Co.,Ltd., Nanjing, 210000, China
[e] Center of LED and Optoelectronic Technologies of NAS Belarus, Minsk, 220090, Belarus
[f] EEMCS Faculty, Delft University of Technology, 2628, Delft, the Netherlands
[g] Fudan Zhangjiang Institute, Shanghai, 201203, China

ARTICLE INFO

Keywords:
White laser lighting
YAG single Crystal
Phosphor-in-borate glass
Surface roughening
High color rendering

ABSTRACT

$Y_3Al_5O_{12}$:Ce^{3+} (YAG:Ce^{3+}) single crystal phosphor (SCP) exhibits high internal quantum efficiency (IQE) and excellent thermal conductivity and stability. Such properties are promising in high-power laser-excited white lighting applications. However, YAG:Ce^{3+} SCP usually shows low luminous flux and color rendering index (CRI, Ra) when excited by a transmissive laser. In this study, a self-designed three-integrating sphere system was established to characerize the optical performances of YAG:Ce^{3+} SCP palates under both the reflective and transmissive 455 nm blue laser excitations. Next, its luminous and color rendering properties under transmissive laser excitation were improved by surface roughening treatment and sintering of a $CaAlSiN_3$:Eu^{2+} (CASN:Eu^{2+}) phosphor-in-borate glass (PiBG) layer. The results revealed that: (1) When the YAG:Ce^{3+} SCP was excited by blue laser, its forward luminous flux was considerably lower than the backward one; (2) Under transmissive excitation, its luminous flux rolled up with the maximum increase rate of 109.19% when the averaged roughness (R_a) increased from 0.35 to 5.40 μm; (3) After sintering the CASN:Eu^{2+} PiBG layer on the roughening YAG:Ce^{3+} SCP, its luminous flux, CRI increased by 31.48% and 117.14%, and its color fidelity index (CFI, R_f) reached up to 82 under the transmissive 3.03 W blue laser excitation.

Author statement

Wei Chen: Experiment; Investigation; Data curation; Writing—original draft, Dunhua Cao: Sample preparation, Yongjun Dong: Sample preparation. Jingkang Xiong: Support in experiment; Funding acquisition. Yuri Trofimov: Supervision; Support in analysis, Sergey Lishik: Supervision; Support in analysis, Guoqi Zhang: Supervision, Jiajie Fan: Conceptualization; Methodology; Writing—review & editing; Supervision; Project administration; Funding acquisition.

1. Introduction

Phosphor-converted white light-emitting diodes (pc-WLEDs) are solid-state lighting devices composed of LED chip and converted phosphor and widely used in many fields because of their high efficiency, long life, and ease of production [1,2]. However, efficiency droop [3] occurs in LED dies, which drastically reduces internal quantum efficiency (IQE) under high driven current. By contrast, laser diodes (LDs) exhibit high IQE under a high driven power density condition [4,5]. Furthermore, LD has low etendue, low beam divergence, and high optical density. Therefore, phosphor-converted white LDs (pc-WLDs) are competitive alternative of pc-WLEDs in high-power and high-brightness applications, such as automotive headlamp, projector and displays [6–8].

Typically, a blue LD is used to excite the phosphor converter to realize white laser lighting; subsequently, the converted light is mixed

* Corresponding author. Institute of Future Lighting, Academy for Engineering & Technology, Fudan University, Shanghai, 200433, China.
E-mail address: jiajie_fan@fudan.edu.cn (J. Fan).

https://doi.org/10.1016/j.jlumin.2022.119225
Received 20 June 2022; Received in revised form 10 August 2022; Accepted 11 August 2022
Available online 17 August 2022

with the transmitted blue laser light to form white light [9]. Phosphor/silicone composite is widely used as a color converter in LEDs, however, it is limited used in pc-WLD as its low thermal stability. The optical density of an LD is extremely high reach up to 6.9 W/mm^2 [10]. Excessive optical density will cause the thermal quenching and carbonization of phosphor/silicone composites [11]. Thus, the color converter used in pc-WLD should satisfy the requirements, such as: (1) high thermal stability, (2) high thermal conductivity, (3) high optical conversion efficiency and (4) high luminance saturation threshold. Currently, the types of laser-excited phosphor include single crystal phosphor (SCP) [12–14], ceramic phosphor [15–17], and phosphor-in-glass (PiG) [18–20].

To satisfy the mechanical fixing of color converter and the independent thermal management for laser source and color converter, a laser excited remote phosphor (LERP) is designed for pc-WLDs [21,22]. Normally, the LERP can be categorized in two types: (1) the transmissive LERP; (2) the reflective LERP. In the transmissive LERP, the relative directions of the laser source and output white light remain the same because the laser light penetrates the color converter. In the reflective LERP, the direction of output white light is opposite to that of the laser source because the light is reflected by a mirror affixed to the back side of color converter. Compared with the reflective LERP, the structure of transmissive LERP is quite simple. However, the optical efficacy of transmissive LERP is lower than that of reflective LERP, thus, the luminous efficiency of reflective pc-WLDs can be several times larger than that of transmissive module at the same operation condition [23,24].

To enhance forward light extraction efficiency, Rondelez et al. proposed a novel optical scheme in which the SCP was fixed on a sapphire half-ball lens [10], which resulted in a 150% improvement in luminous flux. Wagner et al. [25] revealed that the photoluminescence intensity of transmissive white laser light source improves with the increase in the roughness of the surface of the phosphor. Kim et al. [26] also observed this phenomenon and postulated that high surface roughness alleviates total internal reflection in phosphor. Wang et al. [27] fabricated cone-shaped microwells array on the light emission surface of YAG:Ce^{3+} phosphor. Compared with untreated sample, the forward yellow light intensity of above scheme increased by 117. Furthermore, an larger improvement of 350% occurred in the phosphor with the TiO_2 photonic crystal layer [28].

SCP exhibit high internal quantum efficiency even under high temperature. For example, the internal quantum efficiency of YAG:Ce^{3+} SCP always remains higher than 97% from room temperature to 250 °C, and it stays higher than 93% at 300 °C [29]. Deng et al. [30] proved that the photoluminescence intensity of YAG:Ce^{3+} SCP increased first, and subsequently decreased with the increase in the Ce^{3+} content from 0.2 to 5.0 at%, with the peak at 1 at%. Furthermore, the thermal conductivity (~14 W/m·K [9]) of SCP is considerably higher than that of ceramic phosphor (4–5 W/m·K [31]) and PiG (~1 W/m·K [31]), which enhances its heat-transfer capability. Furthermore, Xu et al. [32] investigated the luminescence saturation behavior of YAG:Ce^{3+} SCP by using a self-deigned setup that can be used to adjust the laser spot size and revealed that YAG:Ce^{3+} SCP exhibit a very high luminance saturation threshold (over 360 W/mm^2). Xu et al. [33] verified that the luminescence saturation threshold of SCP was superior to that of ceramic phosphor. Therefore, YAG:Ce^{3+} SCP is considered as a potential candidate in future high-power pc-wLD. Cantore et al. [12] revealed a crystal pc-wLD with the luminous flux of 1100 lm; however, its CRI was only 57. Because of inadequate red light emission, Ce^{3+}-doped SCP with the yellow-green light emission does not exhibit a favorable performance in CRI. Zhang et al. [13] synthesized a Eu^{3+}- and Ce^{3+}-doped YAG SCP. For the red light emission of Eu^{3+}, YAG: Ce^{3+}, Eu^{3+} SCP obtained a high CRI of 87. Arjoca et al. [14] achieved a white laser light with a CRI of more than 90 by combining SCP with commercial red phosphor. Furthermore, because the red LD can provide red light, another method to improve CRI is using both blue and red LDs as the excitation light sources [34].

Most of current researches focused on improving the luminous efficacy and the CRI of YAG:Ce^{3+} SCP separately. However, limited studies have focused on the simultaneous improvement of the two crucial factors. In this study, the optical performances of YAG:Ce^{3+} SCP were characterized using a self-designed three-integrating sphere system, a new method to improve both the luminous flux and CRI simultaneously was proposed and validated. The rest of this study is organized as follows: Section 2 introduces the samples preparation and experiments setups. The luminous performance characterization and its improvement method are described in Section 3. Finally, the concluding remarks are presented in Section 4.

2. Sample preparation and experiments

In this section, the sample preparation processes and the material characterization methods were introduced.

2.1. Sample preparation

Fig. 1(a) displays the preparation process of YAG:Ce^{3+} SCPs by using the Czochralski method. The detailed procedure are list as follows: (1) weighing the commercial raw materials with a high purity of 99.99%: Al_2O_3, Y_2O_3, CeO_2, according the stoichiometric ratio of $(Ce_{0.08}Y_{0.92})_3Al_5O_{12}$; (2) mixing the raw materials by using a blender; (3) heating the mixture at 1100 °C in a crucible; (4) growing the crystals in the furnace with the rate of 1 mm/h; (5) obtaining the YAG:Ce^{3+} single crystal phosphor rod with a Ce^{3+} concentration of 1.2 mol%. The rod was then cut into YAG:Ce^{3+} crystal phosphor plates (SCP) with various thicknesses as test samples. Next, the test samples with thicknesses of 0.8, 1.0, 1.2, 1.4, and 1.6 mm were obtained through well-controlled polishing with 1000 grit abrasive paper. Lower grit abrasive papers of 80, 240, 320, and 500 grit were used for polishing to acquire the plate samples with higher averaged roughness (R_a).

To improve CRI, a CASN:Eu^{2+} PiBG layer was sintered on the surface of the YAG:Ce^{3+} SCP plate. The preparation process is displayed in Fig. 1 (b). First, the analytically pure terpincol and ethocel mixed in a mass ratio of 24:1 were stirred for 30 min in a water bath at 80 °C to form the transparent organic solution carrier. Second, the carrier and CASN:Eu^{2+} PiBG powder at a mass ratio of 3:2 were fully mixed to produce PiBG paste. The PiBG powder is composed of commercial CASN:Eu^{2+} red phosphor and low melting borate glass. Next, the PiBG paste was stencil printed onto one side of YAG:Ce^{3+} SCP plate, the thickness of PiBG layer is 0.15 mm. Third, the YAG:Ce^{3+} SCP plate with CASN:Eu^{2+} PiBG paste was placed in a temperature chamber at 190 °C for 20 min to remove the organic solvent. Then, it was sintered in a muffle furnace under highest temperature of 500 °C for 30mins, the sintering profile is displayed in Fig. 1(b). Finally, after being cooled to room temperature, the YAG:Ce^{3+} single crystal phosphor plate with CASN:Eu^{2+} PiBG (SCP-PiBG) samples were obtained.

2.2. Experiments setups

In this study, a blue laser module with peak wavelength at 445 nm was used as the excitation light source. The optical power output of the laser module ranged from 0.6 to 3.3 W, and the spot size on phosphor was approximately 2 × 4 mm^2 [11]. The luminous performances including spectral power distribution (SPD), luminous flux, correlated color temperature (CCT) and CRI of prepared test samples under both transmissive and reflective excitations were characterized using a self-designed three-integrating sphere system. In transmissive excitation, the test samples were placed between the first and second integrating spheres through a transmissive fixture, as displayed in Fig. 2(a). The first, second, and third integrating spheres were used to collect the reflected, transmitted, and collimated lights accordingly. In reflective excitation, the test samples were placed at the light outlet of the first integrating sphere through the reflective fixture that was coated with a film of silver for a high reflectivity, as displayed in Fig. 2(b). The real

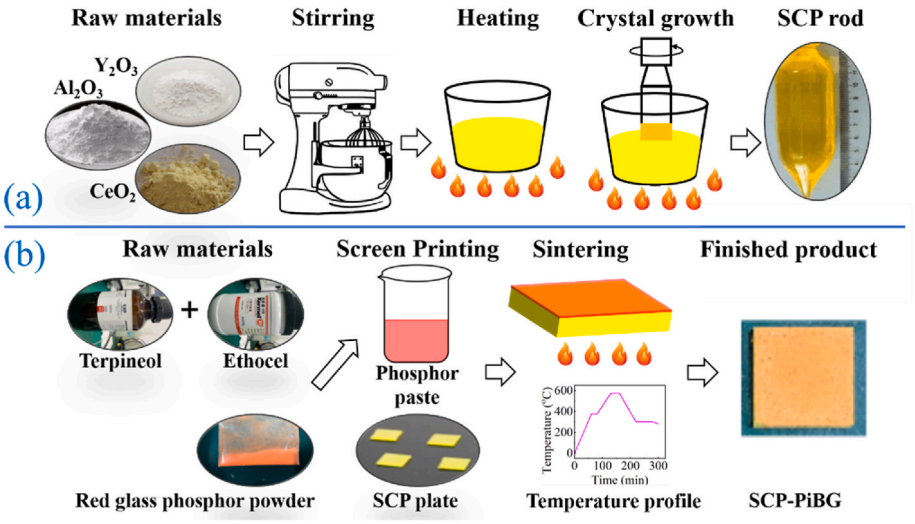

Fig. 1. Sample preparation process: (a) YAG:Ce^{3+} SCP plate; (b) sintering a CASN:Eu^{2+} PiBG layer.

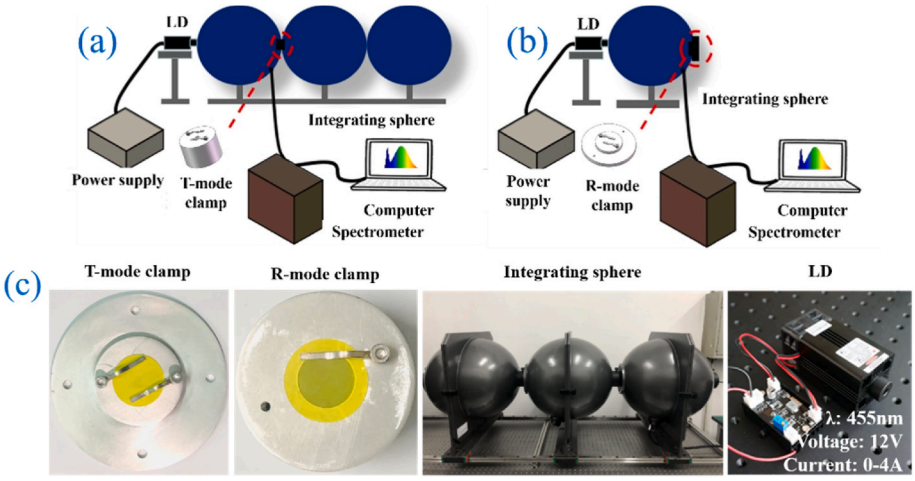

Fig. 2. The self-designed three-integrating sphere system: (a) transmissive excitation; (b) reflective excitation; (c) setups.

pictures of measurement setups are shown in Fig. 2(c).

Furthermore, the R_a value and microstructure of the samples were tested using a roughness tester (LEEB451, China) and scanning electron microscopy (SEM) (Su8010 Hitachi, Japan), respectively.

3. Results and discussion

3.1. Optical performance analysis on YAG:Ce^{3+} SCP plate

Fig. 3 describes the effect of thickness on the luminous flux, luminous efficiency, CCT, and CRI of the YAG:Ce^{3+} SCP under reflective laser excitation. The test samples were double-side polished through 1000 grit abrasive paper. In Fig. 3(a), because the thicknesses of test samples increase from 0.8 to 1.6 mm, the luminous flux rose first, and reached the maximum at 1.4 mm, and subsequently decreased. It is indicated that heavy thickness elongates the optical path length of light penetrating through the test sample, which increases the absorption probability of blue laser by Ce^{3+}. The absorbed light is proportionally converted to the yellow light, which contributes to the lumen flux improvement. As the converted light can also be re-absorbed by Ce^{3+}, excessive optical path length causes additional optical energy loss. Therefore, 1.4 mm is considered as an optimal thickness for the prepared YAG:Ce^{3+} SCP plate under reflective excitation in terms of light outputs. As displayed in Fig. 3(b), the luminous efficiency tended to grow with the increase of laser optical power; however, the increment gradually decreased. The sample with a thickness of 1.4 mm exhibited a peak luminous efficiency of 149.89 lm/W under 3.03 W reflective laser excitation with a luminous flux of 454.18 lm. Previous studies [6,12,23] also revealed that the luminous efficiency of LERP could be saturated through the increase first and subsequently decrease with the increase in the laser power. Accordingly, 3.03 W is lower than the power saturation of the test samples.

The influence of thickness on the chromatic performances of YAG:Ce^{3+} SCP plates is displayed in Fig. 3(c) and (d). With the increase in the thickness, the CCTs of test samples decreased because of the increased yellow light. Their CRIs at all conditions were lower than 55 because of the following reasons: first, the emission of YAG:Ce^{3+} SCP was short of red light; furthermore, most blue laser light was absorbed, only a small part of blue light was released by reflection. This phenomenon was obvious in the heavy-thickness test samples, and laser power exerts a weak influence on chromatic performances.

Fig. 4 displays the optical and chromatic performances of YAG:Ce^{3+} SCP plates versus the thickness under transmissive excitation. The effect of the thickness on lumen performance measured both in 1st and 2nd integrating spheres under transmissive excitation was similar to that under reflective excitation. However, a slight increase in luminous flux

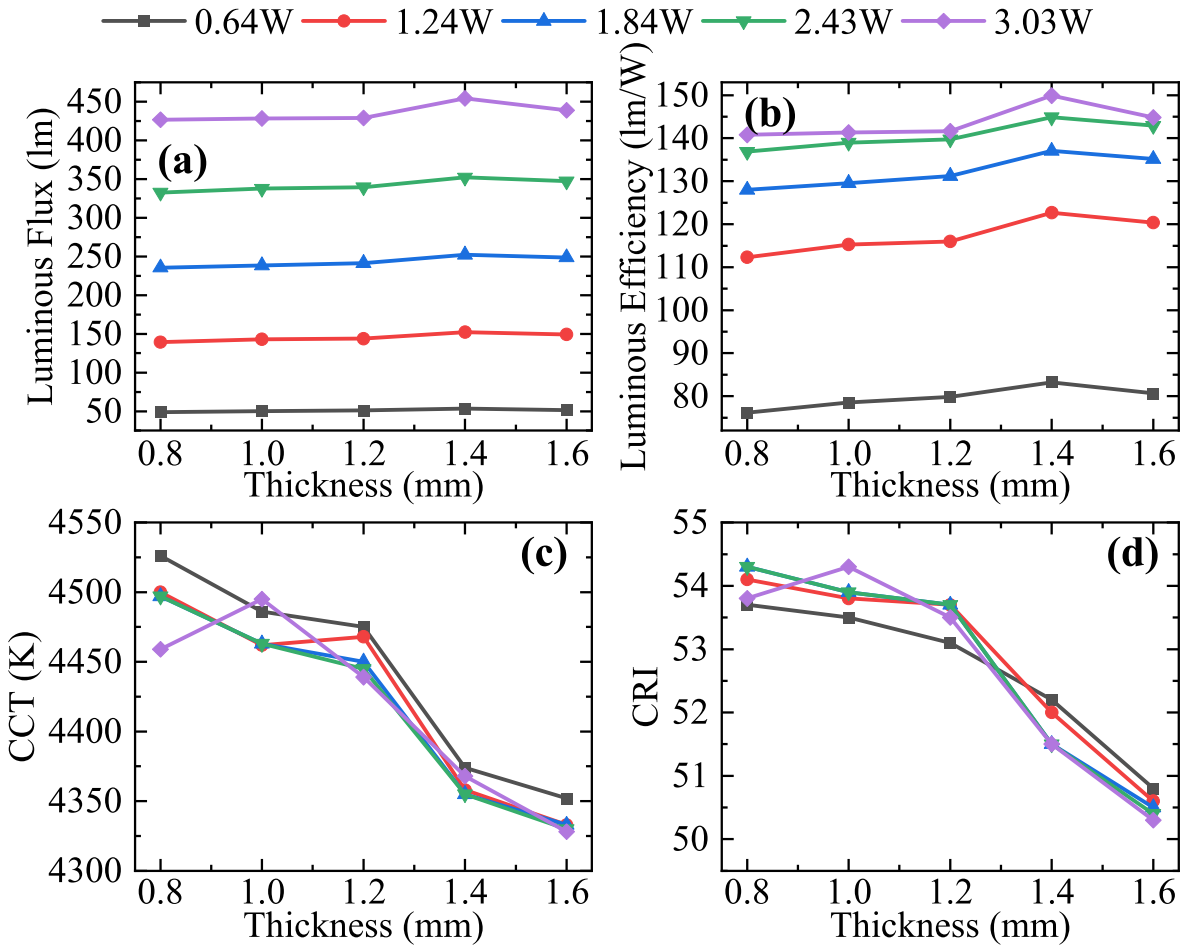

Fig. 3. (a) Luminous flux, (b) luminous efficiency, (c) CCT, and (d) CRI *v.s.* Thickness of the prepared YAG:Ce^{3+} SCP plate under reflective laser exaction.

was observed from 1.4 to 1.6 mm because the optical path length under transmissive excitation was less than that under reflective excitation. The difference in the path length also explained the cause of the luminous flux under reflective excitation being higher than the sum of luminous fluxes measured in all three integrating spheres under transmissive excitation.

The forward luminous flux measured in the 2nd integrating sphere was expected in transmissive excitation application, which was considerably lower than the backward luminous flux measured in 1st integrating sphere. This phenomenon can be attributed to two reasons: first, after the light was captured by Ce^{3+}, the converted light was mostly directed into backward direction, as illustrated in previous studies [11, 23,24]. Second, a large portion of the light escaped from the lateral surface for the total internal reflection. Because the refractive index of the YAG:Ce^{3+} SCP ($n_{SCP} = 1.84$) was larger than that of air ($n_{air} = 1$), only the rays with angles of incidence less than the critical angle (θ_c) could escape from the forward surface; if not, the rays are reflected and escape from lateral surface, as displayed in Fig. 5. The critical angle (θ_c) is merely 33°, which is calculated from the following equation:

$$\theta_c = arcsin\frac{n_{air}}{n_{SCP}} \quad (1)$$

3.2. Luminous flux enhancement via surface roughening

To investigate the effect of surface roughness on the luminous flux, the YAG:Ce^{3+} SCP plates with four R_a values were prepared. One side of the four samples was polished with 1000 grit abrasive paper, another side of the samples was polished with 80, 240, 320, and 500 grit abrasive paper, respectively. Their appearances, surface microstructure (500-fold SEM images) and R_a values are displayed in Fig. 6. It is indicated that the R_a values varied from 0.035 to 5.401 μm depending on the grit size of the abrasive paper. The sample's appearances changed to be less transparent as the R_a value increased. The R_a values in two sides of the roughing samples were different considerably: one sides were all 0.035 μm and the rougher sides were 0.35, 0.99, 1.84, and 5.40 μm, respectively.

In transmissive excitation, the rougher surface can function as the light-emitting surface (denoted by E-model) and light-incident surface (denoted by I-model), as shown in Fig. 8. The luminous flux and its increasing rate under 3.03 W blue laser transmissive excitation are displayed in Fig. 7. In the E-model, the luminous flux was rolled up as the R_a value increased from 0.35 to 5.40 μm. The maximum luminous flux increased to 71.04 lm with a 98.05% increase compared with the sample whose double sides were polished by 1000 grit abrasive paper. As displayed in Fig. 8(a), the roughing surface can lower the incidence angles of rays, which enlarges the escape probability of the rays from the surface. In the I-model, the effect of R_a on the luminous performance was similar to that in the E-model. The maximum luminous flux was 75.15 lm with an increasing of 109.51%. As displayed in Fig. 8(b), after the rays penetrated to the rough surface, beam angle of rays will be increased for the diffuse reflection at the surface. This results in a higher capturing possibility of the blue laser by Ce^{3+}.

3.3. CRI enhancement via sintering a CASN:Eu^{2+} PiBG layer

To improve the CRI of the prepared YAG:Ce^{3+} SCP plates, a 1.4 mm sample whose both sides' R_a values were 0.035 and 5.40 μm, respectively, was used for further processing. A layer of CASN: Eu^{2+} PiBG was sintered on the smoother side (R_a = 0.035 μm) of the sample, and the

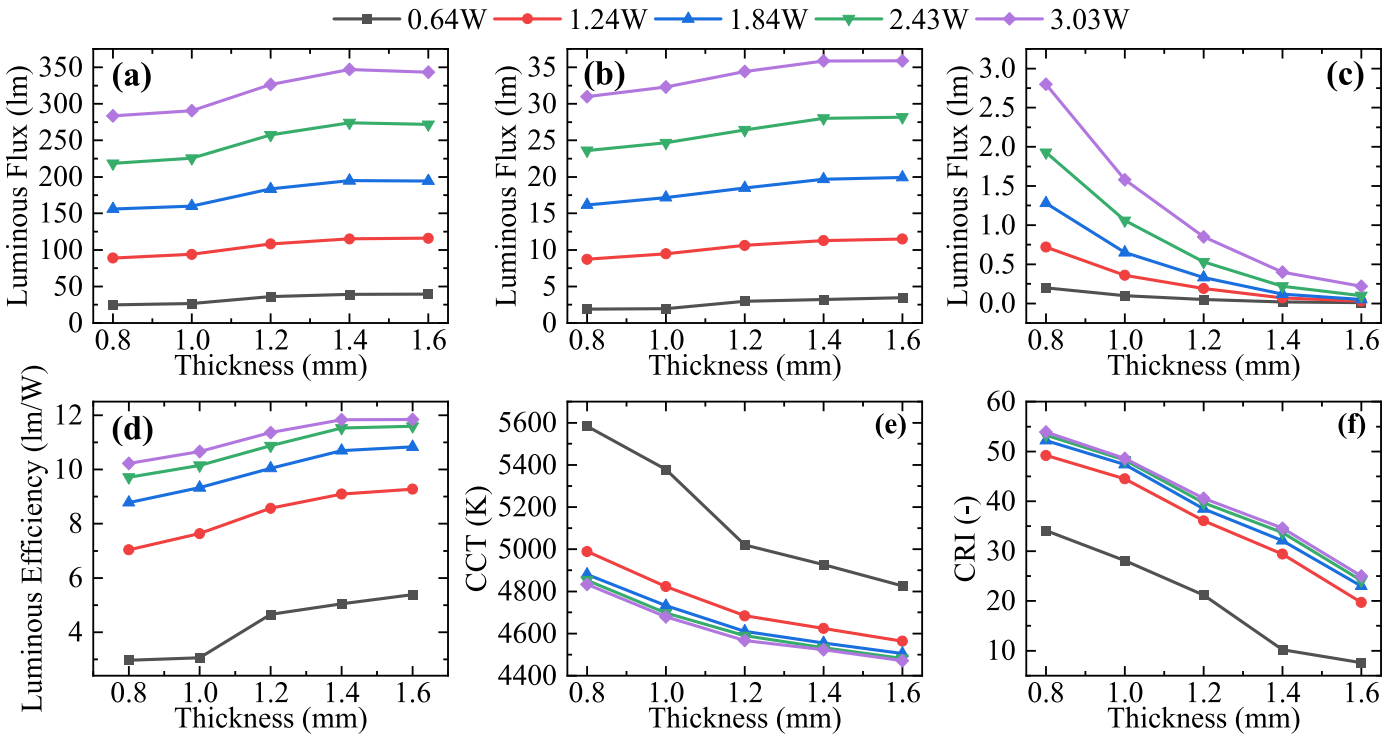

Fig. 4. Optical and chromatic performances *v.s.* Thickness of the prepared YAG:Ce^{3+} SCP plate under transmissive laser excitation: (a) luminous flux measured in the 1st integrating sphere; (b) luminous flux measured in the 2nd integrating sphere; (c) luminous flux measured in the 3rd integrating sphere; (d) luminous efficiency measured in the 2nd integrating sphere; (e) CCT measured in the 2nd integrating sphere; (f) CRI measured in the 2nd integrating sphere.

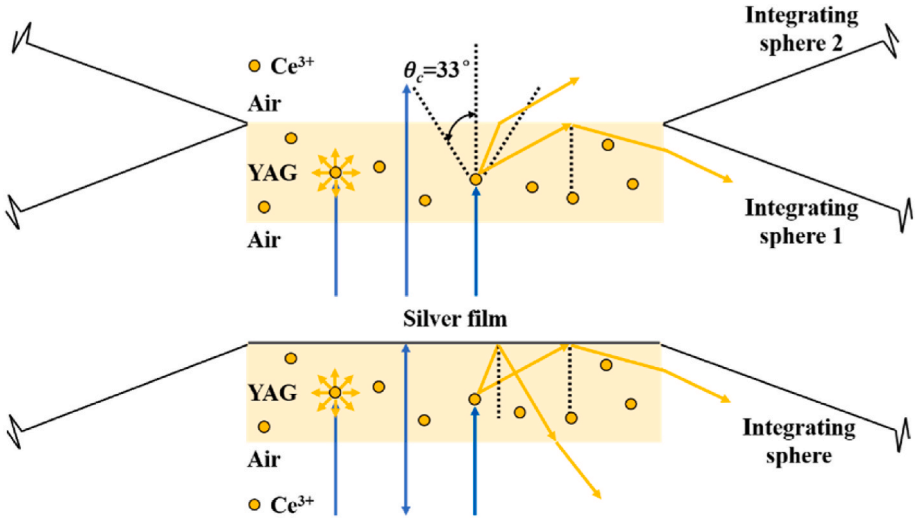

Fig. 5. Schematic illustrations of the ray's pathways in a YAG:Ce^{3+} SCP plate under transmissive and reflective laser exactions.

treated sample was marked as SCP-PiBG. In the transmissive excitation, the PiBG layer worked as both light-emitting surface and light-incident surface, denoting by the SCP-PiBG-I-model and SCP-PiBG-E-model, respectively. Table 1 presents the forward luminous performances of various samples under the transmissive 3.03 W blue laser excitation, and their SPDs are displayed in Fig. 9. For the SCP sample with R_a values of two sides are 0.035 μm, only a little of blue light was observed in the forward output light, which results in a lower CRI of 35. Regarding the SCP sample with R_a = 5.40 μm, the roughening treatment enhances the blue light emission and yellow light emission, which enhances the luminous and CRI simultaneously.

As the CASN: Eu^{2+} PiBG layer increased red light emission to the forward output light, their CRIs were improved considerably. For SCP-PiBG, the measured CRIs in both I-model and E-model were 70 and 76, respectively. However, the CASN: Eu^{2+} PiBG layer decreased the luminous efficacy as the low conversion efficacy of CASN: Eu^{2+} phosphor and the low spectral luminous efficacy of red light emission [35, 36]. Compared with SCP sample with R_a = 0.035 μm, the luminous flux and CRI of SCP-PiBG-I sample increased by 31.48% and 117.14%, respectively.

Color rendering index proposed by the Commission Internationale de l'Eclairage (CIE) was used to describe the color rendering properties of light sources. Nonetheless, it is insufficient in depicting the perceived color fidelity and the subjective aspects of color perception. Therefore, color fidelity Index (R_f) was presented by the Illuminating Engineering Society of North America (IES) to predict the perceived color fidelity, the

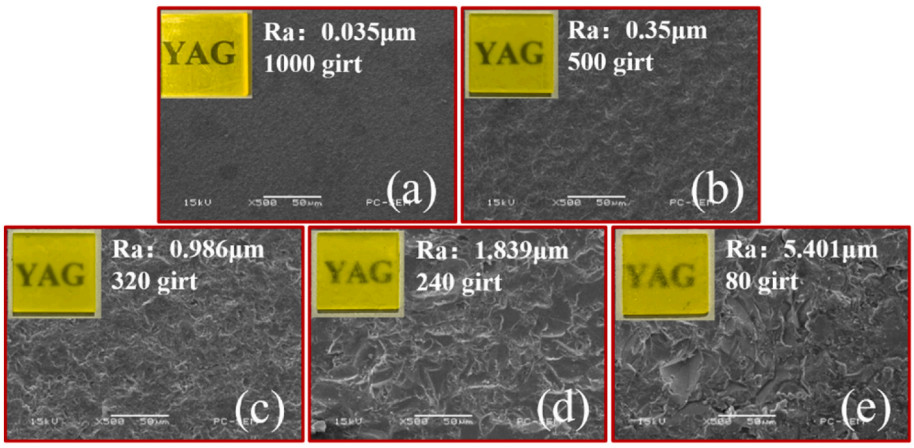

Fig. 6. The appearance, surface microstructure and Ra of the prepared YAG:Ce^{3+} SCP plate under different girt abrasive polishing: (a) 1000 git; (b) 500 girt; (c) 320 girt; (d) 240 girt; (e) 80 girt.

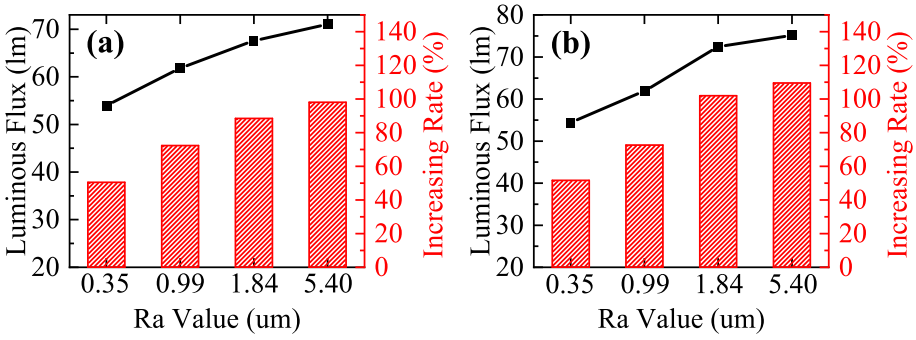

Fig. 7. The measured luminous flux *v.s.* Surface roughness of the prepared YAG:Ce^{3+} SCP plate: (a) E-model; (b) I-model.

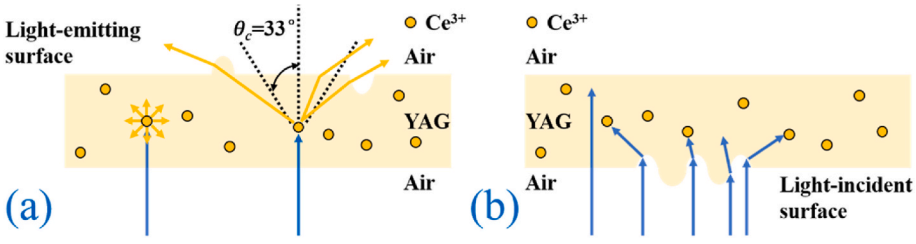

Fig. 8. Schematic illustrations of the ray's pathways in YAG:Ce^{3+}:(a) E model; (b) I model.

Table 1
Comparison of luminous fluxes, CRIs and CFIs of YAG:Ce^{3+} SCP plates sintered with CASN:Eu^{2+} PiBG layer under the transmissive 3.03 W blue laser excitation.

Sample models	Luminous flux (lm)	Improvement ratio of luminous flux (%)	CRI, R_a	Improvement ratio of CRI (%)	CFI, R_f
SCP-0.035 μm	35.90	/	35	/	N/A
SCP-5.40 μm-E	71.00	97.77	61	74.29	69
SCP-5.40 μm-I	75.10	109.19	61	74.29	68
SCP-PiBG-E	47.40	32.03	70	100	78
SCP-PiBG-I	47.20	31.48	76	117.14	82

measurement of R_f is based on 99 standard color samples that represent the world of possible colors [37–41]. R_f is calculated by following equations:

$$R'_f = 100 - 6.73\left[\frac{1}{99}\sum_{i=1}^{99}\left(\Delta E_{Jab,\,i}\right)\right] \quad (2)$$

$$R_f = 10ln\left[\exp\left(\frac{R'_f}{10}\right)+1\right] \quad (3)$$

in which $\Delta_{Jab,i}$ is the color difference between the measured light and the ith reference light sample (CAM02UCS color space). For SCP-PiBG, the measured R_f in both I-model and E-model were 78 and 82, respectively, which are higher than the values of SCP-0.54 μm. The chromaticity of the SCP-0.035 μm is too far off blackbody locus, and the R_f can not be calculated.

Fig. 10 displays the light distributions of all prepared samples list in Table 1 on a white wall. Warm white light could be obtained by using the a transmissive 3.03 W blue laser excited YAG:Ce^{3+} SCP plates

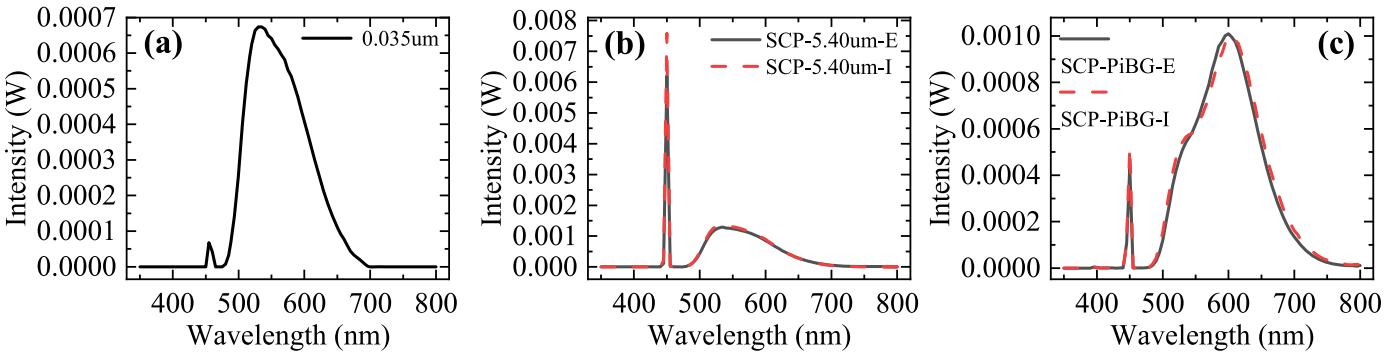

Fig. 9. The SPDs of different samples under transmissive 3.03 W blue laser excitation: (a) SCP-0.035 μm; (b) SCP-5.40 μm; (c) SCP-PiBG.

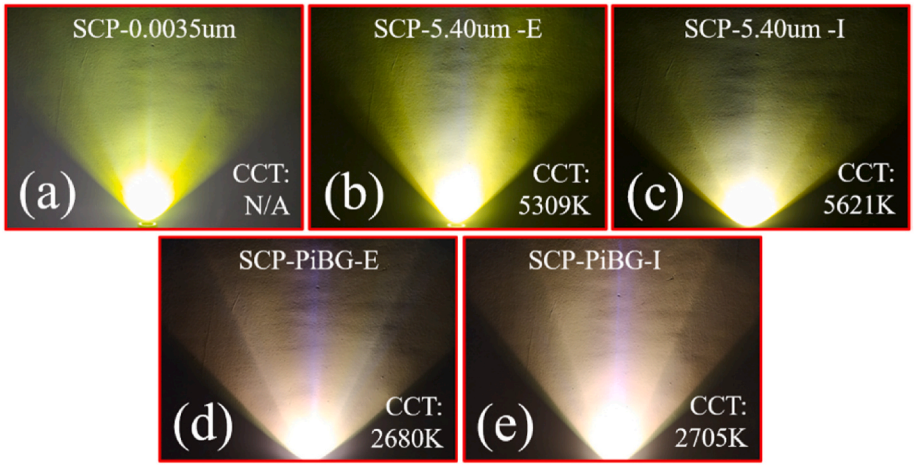

Fig. 10. The light distributions on a white wall: (a) SCP-0.035 μm; (b) SCP-5.40 μm-E; (c) SCP-5.40 μm-I; (d) SC-PiBG-E; (e) SC-PiBG-I.

sintered a CASN:Eu^{2+} PiBG layer. However, there were still some blue laser rays leaked in the middle of the spot.

4. Conclusion

In this study, luminous flux and color rendering of YAG:Ce^{3+} single crystal phosphor plates were analyzed based on under both reflective and transmissive blue laser excitations. Next, the surface roughening treatment was proposed to improve the luminous flux of prepared YAG:Ce^{3+} SCP plates. Finally, a CASN: Eu^{2+} PiBG layer was sintered on the YAG:Ce^{3+} SCP plate to enhance its luminous flux and CRI simultaneously. The results revealed that: (1) the luminous saturation was in the YAG:Ce^{3+} SCP plate with thickness of 1.4 mm under reflective excitations, however, from 1.4 to 1.6 mm, a slight increase in luminous flux was observed in transmissive excitation; (2) under reflective excitation, its converted lights were mostly directed into the backward direction after being captured by Ce^{3+}, which attributed to a larger luminous flux than that under transmissive excitation; (3) the luminous flux rolled up as the surface roughness increased regardless of the rougher surface functioned as light-emitting or light-incident surface; and (4) after a CASN: Eu^{2+} PiBG layer was sintered on the roughening treated YAG:Ce^{3+} SCP plate, the luminous flux and CRI can be both enhanced by 31.48% and 117.14%, respectively, and a warm white lighting with $R_f = 82$ was obtained. However, the non-uniformity of light distribution attributed to the blue laser leakage should be improved in the future study, i.e. laser spot optimization, designs of arch-shaped color converter or surface micro-structure.

Funding

The work described in this paper was partially supported by the National Natural Science Foundation of China (51805147), National Key R&D Program of China (2021YFB3601000, 2021YFB3601005), State Key Laboratory of Applied Optics (SKLAO2022001A01), Shanghai Science and Technology Development Foundation (21DZ2205200) and Shanghai Pujiang Program (2021PJD002).

Declaration of competing interest

The authors declare that they have no known competing financial interests or personal relationships that could have appeared to influence the work reported in this paper.

Data availability

The data that has been used is confidential.

References

[1] A. Kar, K. Kundu, H. Chattopadhyay, R. Banerjee, White light emission of wide-bandgap silicon carbide: a review, J. Am. Ceram. Soc. 105 (2022) 3100–3115.
[2] S. Khan, M. Usman, S. Ali, Perspective on light-fidelity and visible light communication, J. Laser Appl. 34 (2022), 011202.
[3] S. Zhou, Z. Wan, Y. Lei, B. Tang, G. Tao, P. Du, X. Zhao, InGaN quantum well with gradually varying indium content for high-efficiency GaN-based green light-emitting diodes, Opt. Lett. 47 (2022) 1291–1294.
[4] H.-c. Yu, Z.-w. Zheng, Y. Mei, R.-b. Xu, J.-p. Liu, H. Yang, B.-p. Zhang, T.-c. Lu, H.-c. Kuo, Progress and prospects of GaN-based VCSEL from near UV to green emission, Prog. Quant. Electron. 57 (2018) 1–19.
[5] C. Zhang, R. ElAfandy, J. Han, Distributed bragg reflectors for GaN-based vertical-cavity surface-emitting lasers, Appl. Sci. 9 (2019).

[6] J. Yang, Z. Liu, B. Xue, J. Wang, J. Li, Research on phosphor-conversion laser-based white light used as optical source of VLC and illumination, Opt. Quant. Electron. 49 (2017) 173.
[7] X. Zhang, J. Yu, J. Wang, B. Lei, Y. Liu, Y. Cho, R.-J. Xie, H.-W. Zhang, Y. Li, Z. Tian, Y. Li, Q. Su, All-inorganic light convertor based on phosphor-in-glass engineering for next-generation modular high-brightness white LEDs/LDs, ACS Photonics 4 (2017) 986–995.
[8] Y. Manabe, M. Ishino, H. Fuji, J. Kinoshita, K. Fujioka, K. Yamamoto, Improvement of color rendering index of BGYR laser illuminants, Opt. Rev. 29 (2022) 267–275.
[9] Y. Ma, X. Luo, Packaging for laser-based white lighting: status and perspectives, J. Electron. Packag. 142 (2019).
[10] N. Rondelez, A. Correia, W. Ryckaert, H. De Smet, D. Cuypers, Y. Meuret, Efficient transmissive remote phosphor configuration for a laser-driven high-luminance white light source, Opt Express 30 (2022) 5107–5120.
[11] Y. Cao, W. Chen, Y. Du, G. Qi, T. Santos, G. Zhang, J. Fan, Luminous performances characterization of YAG: Ce3+ phosphor/silicone composites using both reflective and transmissive laser excitations, IEEE Photonics Journal 14 (2022) 1–6.
[12] M. Cantore, N. Pfaff, R.M. Farrell, J.S. Speck, S. Nakamura, S.P. DenBaars, High luminous flux from single crystal phosphor-converted laser-based white lighting system, Opt Express 24 (2016) A215–A221.
[13] J. Zhang, G. Gu, X. Di, W. Xiang, X. Liang, Optical characteristics of Ce,Eu:YAG single crystal grown by Czochralski method, J. Rare Earths 37 (2019) 145–150.
[14] S. Arjoca, E.G. Víllora, D. Inomata, K. Aoki, Y. Sugahara, K. Shimamura, Ce:(Y1-x Lux)3Al5O12 single-crystal phosphor plates for high-brightness white LEDs/LDs with high-color rendering (Ra > 90) and temperature stability, Mater. Res. Express 1 (2014), 025041.
[15] T. Wang, K. Qin, X. Wang, Modeling and Monte Carlo simulation on photothermal effect in Gd3Al3Ga2O12:Ce3+/Y3Al5O12:Cr3+ layered composite ceramic, J. Am. Ceram. Soc. 105 (2022) 4071–4088, n/a.
[16] Q.-Q. Zhu, Y. Meng, H. Zhang, S. Li, L. Wang, R.-J. Xie, YAGG:Ce phosphor-in-YAG ceramic: an efficient green color converter suitable for high-power blue laser lighting, ACS Applied Electronic Materials 2 (2020) 2644–2650.
[17] Z. Liu, S. Li, Y. Huang, L. Wang, Y. Yao, T. Long, X. Yao, X. Liu, Z. Huang, Composite ceramic with high saturation input powder in solid-state laser lighting: microstructure, properties, and luminous emittances, Ceram. Int. 44 (2018) 20232–20238.
[18] Y. Peng, Y. Mou, Q. Sun, H. Cheng, M. Chen, X. Luo, Facile fabrication of heat-conducting phosphor-in-glass with dual-sapphire plates for laser-driven white lighting, J. Alloys Compd. 790 (2019) 744–749.
[19] H. Wang, Y. Mou, Z. Lei, Q. Wang, Y. Peng, M. Chen, Enhanced color quality of phosphor-converted white laser diodes through bicolor phosphor-in-glass, IEEE Trans. Electron. Dev. 68 (2021) 5652–5655.
[20] J. Zhang, H. Yang, Y. Zhang, X. Liu, Y. Zhang, Y. Liang, H. Li, B. Ma, X. Liang, W. Xiang, Stable phosphor-in-glass realizing ultrahigh luminescence efficiency for high-power laser-driven lighting, Appl. Phys. Lett. 119 (2021), 023301.
[21] Y. Ma, W. Lan, B. Xie, R. Hu, X. Luo, An optical-thermal model for laser-excited remote phosphor with thermal quenching, Int. J. Heat Mass Tran. 116 (2018) 694–702.
[22] A. Lenef, J.F. Kelso, J. Serre, A.A. Kulkarni, D. Kinkenon, M. Avison, Co-sintered ceramic converter for transmissive laser-activated remote phosphor conversion, Appl. Phys. Lett. 120 (2022), 021104.
[23] Y. Ma, M. Wang, X. Luo, A comparative study of reflective and transmissive phosphor-converted laser-based white lighting, in: 2018 17th IEEE Intersociety Conference on Thermal and Thermomechanical Phenomena in Electronic Systems, ITherm, 2018, pp. 773–777.
[24] N. Trivellin, M. Yushchenko, M. Buffolo, C. De Santi, M. Meneghini, G. Meneghesso, E. Zanoni, Laser-based lighting: experimental analysis and perspectives, Materials 10 (2017).
[25] A. Wagner, B. Ratzker, S. Kalabukhov, N. Frage, Enhanced external luminescence quantum efficiency of ceramic phosphors by surface roughening, J. Lumin. 213 (2019) 454–458.
[26] J.S. Kim, S.K. Eswaran, O.H. Kwon, S.J. Han, J.H. Lee, Y.S. Cho, Enhanced luminescence characteristics of remote yellow silicate phosphors printed on nanoscale surface-roughened glass substrates for white light-emitting diodes, Adv. Opt. Mater. 4 (2016) 1081–1087.
[27] S. Wang, Y. Li, L. Feng, L. Zhang, Y. Zhang, X. Su, W. Ding, F. Yun, Laser patterning of Y3Al5O12:Ce3+ ceramic phosphor platelets for enhanced forward light extraction and angular color uniformity of white LEDs, Opt Express 24 (2016) 17522–17531.
[28] A. Mao, R.F. Karlicek, Surface patterning of nonscattering phosphors for light extraction, Opt. Lett. 38 (2013) 2796–2799.
[29] M.H. Balci, F. Chen, A.B. Cunbul, Ø. Svensen, M.N. Akram, X. Chen, Comparative study of blue laser diode driven cerium-doped single crystal phosphors in application of high-power lighting and display technologies, Opt. Rev. 25 (2018) 166–174.
[30] W. Deng, Z. Chen, Y. Meng, X. Cao, D. Xiong, Y. Huang, Micro-defects and optical properties of YAG:Ce crystals prepared by optical floating zone method, Int. J. Mod. Phys. B 31 (2017), 1744068.
[31] S. Li, L. Wang, N. Hirosaki, R.-J. Xie, Color conversion materials for high-brightness laser-driven solid-state lighting, Laser Photon. Rev. 12 (2018), 1800173.
[32] J. Xu, A. Thorseth, C. Xu, A. Krasnoshchoka, M. Rosendal, C. Dam-Hansen, B. Du, Y. Gong, O.B. Jensen, Investigation of laser-induced luminescence saturation in a single-crystal YAG:Ce phosphor: towards unique architecture, high saturation threshold, and high-brightness laser-driven white lighting, J. Lumin. 212 (2019) 279–285.
[33] J. Xu, Y. Yang, Z. Guo, D.D. Corell, B. Du, B. Liu, H. Ji, C. Dam-Hansen, O. B. Jensen, Comparative study of Al2O3-YAG:Ce composite ceramic and single crystal YAG:Ce phosphors for high-power laser lighting, Ceram. Int. 46 (2020) 17923–17928.
[34] C.E. Reilly, G. Lheureux, C. Cozzan, E. Zeitz, T. Margalith, S. Nakamura, R. Seshadri, C. Weisbuch, S.P. DenBaars, Transmission geometry laser lighting with a compact emitter, Phys. Status Solidi 217 (2020), 2000391.
[35] Q. Huang, P. Sui, F. Huang, H. Lin, B. Wang, S. Lin, P. Wang, J. Xu, Y. Cheng, Y. Wang, Toward high-quality laser-driven lightings: chromaticity-tunable phosphor-in-glass film with “phosphor pattern” design, Laser Photon. Rev. 16 (2022), 2200040.
[36] H. Chima, N. Shiokawa, K. Seto, K. Takahashi, N. Hirosaki, T. Kobayashi, E. Tokunaga, Thermal relaxation spectra for evaluating luminescence quantum efficiency of CASN:Eu2+ measured by balanced-detection sagnac-interferometer photothermal deflection spectroscopy, Appl. Sci. 10 (2020).
[37] M. Wei, M. Royer, H.P. Huang, Perceived colour fidelity under LEDs with similar Rf but different Ra, Light. Res. Technol. 51 (2019) 858–869.
[38] J. Kowalska, I. Fryc, Colour rendition quality of typical fluorescent lamps determined by CIE colour fidelity index and colour rendering index, Przeglad Elektrotechniczny 95 (2019) 94–97.
[39] R. Supronowicz, J. Fan, M. Listowski, A. Watras, I. Fryc, Application of different metrics for describing light color quality of white LED, Photonics Letters of Poland 13 (2021) 31.
[40] M.P. Royer, Comparing measures of average color fidelity, Leukos 14 (2018) 69–85.
[41] S. Jost, C. Cauwerts, P. Avouac, CIE 2017 color fidelity index Rf: a better index to predict perceived color difference? J. Opt. Soc. Am. Opt Image Sci. Vis. 35 (2018) B202–B213.